K$_4$Nb$_6$O$_{17}$ layered hexaniobate: revisiting the proton-exchanged reaction

Mariana Pires Figueiredo[1] , Vera Regina Leopoldo Constantino[1+]

1. University of São Paulo, Institute of Chemistry, São Paulo, Brazil.

+Corresponding author: Vera Regina Leopoldo Constantino, **Phone:** +551130919152, **Email address:** vrlconst@iq.usp.br

ARTICLE INFO

ABSTRACT: The layered hexaniobate of K$_4$Nb$_6$O$_{17}$ composition and its derivatives comprise nanostructured materials that exhibit suitable properties for application in catalysis, electrochemistry, and energy, for instance. The exchange of K$^+$ cations to obtain the acidic or protonic niobate form is the main route to originate appropriate precursors to promote the hexaniobate exfoliation, yielding a dispersion of thin layers (2D particles) that can be scrolled under exclusive conditions. Hexaniobate presents two regions

(I and II), being the former considered more accessible than region II. In this work, the proton exchange efficiency of the K$_4$Nb$_6$O$_{17}$ was investigated by thermogravimetric analysis coupled to mass spectrometry (TGA-MS) and metal analysis by inductively coupled plasma spectroscopy (ICP). The products of thermal decomposition profile of the H$_x$K$_{(4-x)}$Nb$_6$O$_{17}$ phase were isolated at defined temperature values and characterized by X-ray diffractometry and Raman spectroscopy. The cation exchange percentages obtained by TGA-MS (68.0%) and by quantification of deintercalated K$^+$ by ICP (64.0%) are similar and endorse that region II can also be modified and, consequently, contribute to the exfoliation process.
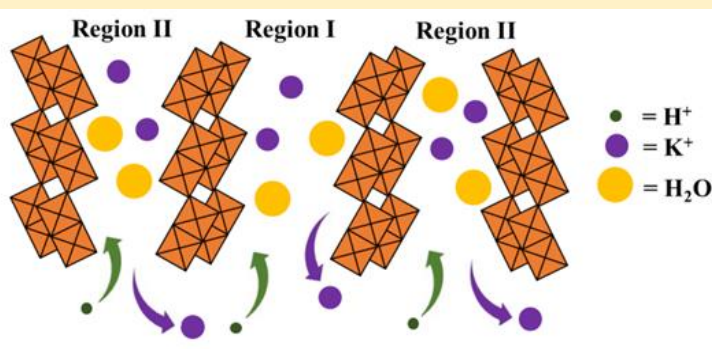
1. Introduction

The interest in layered hexaniobates is motivated by their physicochemical properties and the possibility of application as precursors for the development of nanostructured materials to attend catalysis (Wei and Nakato, 2009), electrochemistry (Elumalai *et al.*, 2021), and energy (Maeda *et al.*, 2009) fields, for instance. Such materials present general formula $A_4Nb_6O_{17} \cdot nH_2O$ (with $A = K^+$, Rb^+, or Cs^+) and orthorhombic unit cell: a = 7.83 Å, b = 32.21 Å, and c = 6.46 Å (Gasperin and Le Bihan, 1980; 1982). The distorted octahedrons $[NbO_6]$ units are bounded by the edges and the vertices, generating layers with structure called ReO_3-type deficient double strand (Bizeto *et al.*, 2006; Rao and Raveau, 1998), as shown in Fig. 1. The three-dimensional structure is formed by the layers stacking in a face-to-face arrangement. Due to the high amount of oxygen atoms coordinated to niobium atoms, hexaniobate presents high layer charge density, which can make the intercalation process by ion exchange reaction (a topotactic reaction) a challenging process. The electroneutrality of the negatively charged layers is maintained by alkali metal cations present in the interlayer region.
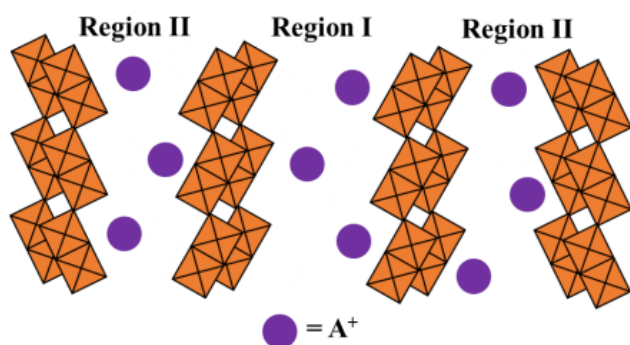
Figure 1. Schematic representation of the layered hexaniobate structure.

One of the most prominent characteristics of $A_4Nb_6O_{17} \cdot nH_2O$ material is the interlayer differentiation, which can be explored to tune its chemical and physical properties. Reported for the first time by Gasperin and Le Bihan (1980), the so-called interlayer I and II regions of the hexaniobate matrix (Fig. 1) present different cations array and behaviors in relation to the hydration process. Ions in the interlayer I can be hydrated, which can made it more accessible than interlayer II.

Consequently, it is supposed that region II is not involved in ion exchange reactions (Kimura *et al.*, 2014; Shiguihara *et al.*, 2010). However, for the $K_4Nb_6O_{17}$ hexaniobate, it is reported that K^+ can be exchanged by multivalent cations in region I but cations exchange in

region II is limited to monovalent cations (Müller-Warmuth and Schöllhorn, 1994).

The exchange of cations to obtain the acidic or protonic niobate form aims to produce precursors able to encapsulate bulky species, such as tetrabutylammonium ion, and support the osmotic swelling facilitating the exfoliation process (Shiguihara *et al.*, 2007). Dispersed exfoliated nanosheets can curl themselves resulting in nanoscrolls with variable diameters, formed according to adjusted experimental conditions. Hence, the reactivity of hexaniobate regarding the layer's separation is affected by the protonation level. Exfoliated nanosheets are investigated for the preparation of thin films targeting coatings or hybrid self-assembled multifunctional systems with a great interest for sensors, among several other applications (Bizeto *et al.*, 2009).

Considering the most studied hexaniobate composition, $K_4Nb_6O_{17}$, the phase resulting from the exchange of K^+ ion by H^+ (or hydronium ion, H_3O^+) is frequently represented by the $H_2K_2Nb_6O_{17}$ formula (Liu *et al.*, 2017; Shiguihara *et al.*, 2010; Silva *et al.*, 2018). However, other works (Guo *et al.*, 2020; Li *et al.*, 2016) have considered proton-exchange values greater than 50%, although chemical elemental quantifications are not provided. In another case, the isolated acid phase was generically expressed as $H_xK_{(4-x)}Nb_6O_{17}$ (Hu *et al.*, 2014). There is no agreement regarding the extension of H^+ intercalation and the quantification of the exchange extension is rarely reported. Thus, the investigation concerning the proton exchange reaction involving the $K_4Nb_6O_{17}$ phase is of interest and required to tune hexaniobate properties.

In this work, the $K_4Nb_6O_{17}$ proton exchange reaction is revisited. Thermogravimetric analysis coupled to mass spectrometry (TGA-MS) was used to assess the proton exchange efficiency of $K_4Nb_6O_{17}$, and the result was compared to the deintercalated amount of K^+ obtained by Inductively Coupled Plasma Optical Emission Spectroscopy (ICP-AES). Additionally, X-ray diffraction (XRD) and Raman spectroscopy were employed to characterize the acidic hexaniobate treated at defined temperature values to better assign the thermal events and, consequently, the extension of the proton exchange.

2. Experimental

2.1 Reagents

Niobium(V) oxide (CBMM – 99,98%, optic degree), potassium carbonate (Merck – p.a.), and nitric acid (Synth – P.A.) were used as received.

2.2 Synthesis of $K_4Nb_6O_{17}$ phase

The potassium layered hexaniobate was synthetized by the ceramic method. Nb_2O_5 and K_2CO_3 solids (with K_2CO_3 in 10 mol% excess related to stoichiometric proportions) were manually ground together, added to a platinum crucible, and heated at 1000 °C in two steps of 5 h. The rate of heating was maintained in 15 ºC min^{-1}. The solid was washed with deionized water by centrifugation cycles for the removal of residual K_2O and then dried at 80 ºC for 24 h.

2.3 Preparation of $H_xK_{(4-x)}Nb_6O_{17}$ phase by ion exchange reaction

The $H_xK_{(4-x)}Nb_6O_{17}$ phase was obtained under mild conditions suspending 1 g of $K_4Nb_6O_{17}\cdot nH_2O$ in 40 mL of 6 mol L^{-1} HNO_3 solution under stirring at 60 °C. After 24 h, the supernatant and the deionized water portions used to wash the solid were transferred to a filter from Millipore Express® plus with 0.22 μm pore diameter. All liquid collected as a filtrate was added to a 250 mL flask and the volume was completed with deionized water; later, the amount of K^+ cation was quantified by chemical analysis.

2.4 Thermal treatment of $H_xK_{(4-x)}Nb_6O_{17}$ sample

Four portions of the $H_xK_{(4-x)}Nb_6O_{17}$ sample were separately added to crucibles and thermal treated at 250, 300, 350, or 400 °C for 30 min.

2.5 Instruments

XRD patterns of $K_4Nb_6O_{17}$ and $H_xK_{(1-x)}Nb_6O_{17}$ powdered samples were recorded in a Rigaku MiniFlex equipment, using Cu anode (1.518 Å), scan range 1.5-70°(2θ), and scan step of 0.015° (2θ)/2s.

Thermogravimetric analysis coupled to mass spectrometry (TGA-MS) was performed in a Netzsch thermalanalyzer model TGA/DSC 490 PC Luxx coupled to an Aëolos 403 C mass spectrometer, using platinum crucible, from room temperature to 600 °C, and heating rate of 10 °C min^{-1} under synthetic air flow of 50 mL min^{-1}.

Raman spectra were recorded in a Bruker FT-Raman (laser wavelength = 1064 nm), at 50 mW and 512 scans, resolution of 4 cm^{-1}, and gain of 32.

ICP-AES analysis of potassium element from the supernatant of the ion exchange reaction was performed in an Spectro Analytical Instruments equipment at the Central Analítica of Instituto de Química (Universidade de São Paulo – USP).

The synthesis of the $K_2Nb_6O_{17}$ phase and the thermal treatment of $H_xK_{(4-x)}Nb_6O_{17}$ sample were proceeded in a Carbolite RHF 1500 furnace.

3. Results and discussion

Figures 2a and 2b show the XRD patterns of $K_4Nb_6O_{17}$ and $H_xK_{(4-x)}Nb_6O_{17}$ samples, respectively, displaying narrow and intense peaks related to the basal spacing, which profiles agree with the literature (Bizeto and Constantino, 2004; Madaro et al., 2011; Nassau et al., 1969). For the $K_4Nb_6O_{17}$ precursor, no reflections concerning the Nb_2O_5 nor K_2O reagents were identified. The positions of the (0$\underline{2n}$0) peaks are in agreement with the tri-hydrated potassium layered hexaniobate. (Bizeto and Constantino, 2004; Nassau et al., 1969; Shiguihara et al., 2007). Basal spacing (d(040)) is equal to 9.36 Å. After the exchange of K^+ ions by H^+ cations, the (040) peak is displaced towards higher angles region in agreement with the intercalation of hydrated H^+/H_3O^+ cations, conducting to the decrease in the basal spacing to 7.97 Å, as shown in Fig. 2b.
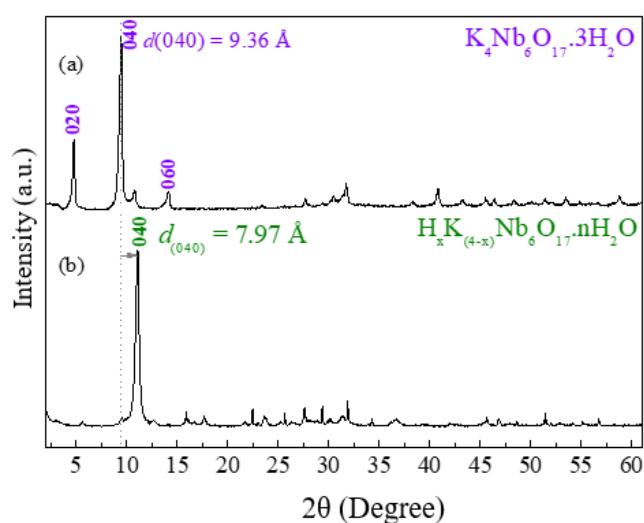
Figure 2. XRD patterns of hydrated (a) $K_4Nb_6O_{17}$ and (b) $H_xK_{(4-x)}Nb_6O_{17}$ samples.

The dehydroxylation process of the $H_xK_{(4-x)}Nb_6O_{17}$ phase was investigated by heating the sample at different temperature values. Figure 3 shows the XRD patterns of the $H_xK_{(4-x)}Nb_6O_{17}$ sample and the thermal treated material at 250, 300, 350, and 400 °C. The increase in the temperature promotes a progressive reduction in the intensity of the (040) peak, already evident for the sample heated at 250 °C, as well as the decrease in the $d(040)$ basal spacing, indicating the partial collapse of the layered structure because de dehydroxylation process.
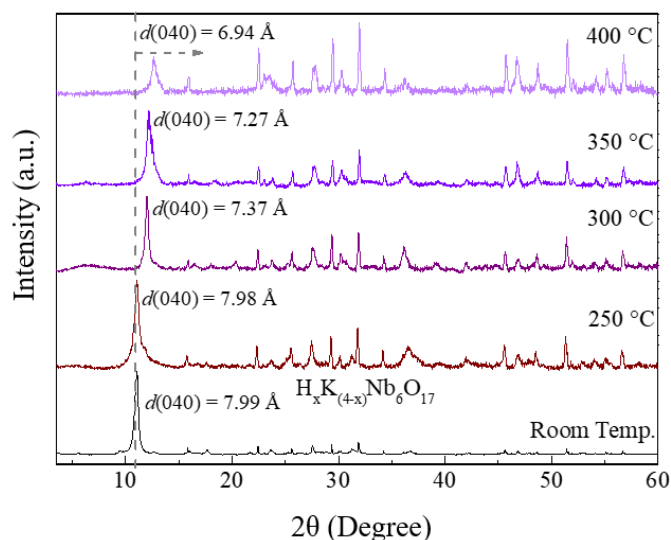
Figure 3. XRD patterns of $H_xK_{(4-x)}Nb_6O_{17}$ sample and the products isolated after the thermal treatment at 250, 300, 350, and 400 °C.
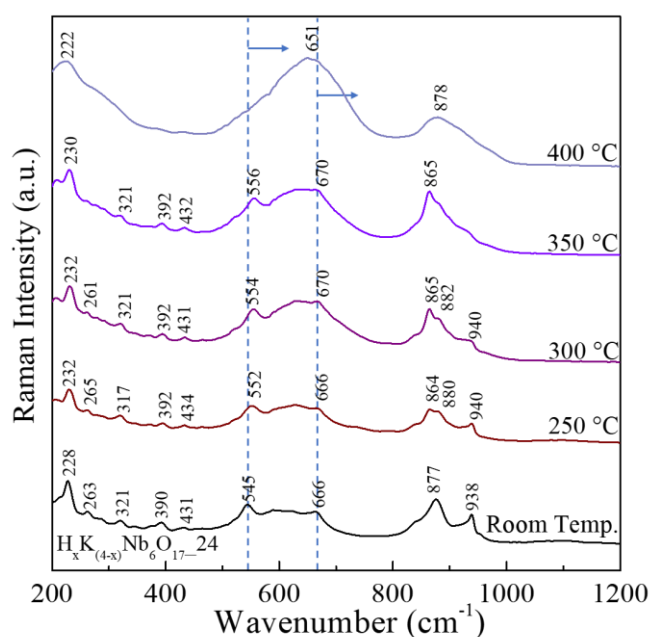
Figure 4 shows the Raman spectra of $H_xK_{(4-x)}Nb_6O_{17}$ and the thermal treated samples. For the nonthermal treated sample, the bands in the $200 - 300$ cm^{-1} region are attributed to the bending of the Nb–O–Nb bond. Slightly-distorted octahedra originate the bands in the $500 - 700$ cm^{-1} range, while the bands between 850 and 1000 cm^{-1} are assigned to highly-distorted [NbO$_6$] units, in which the terminal Nb–O groups present double bond character (Bizeto *et al.*, 2010). Increasing the temperature value, the band around 940 cm^{-1} progressively decreases in intensity because of the condensation of the terminal Nb-O groups. Bands at around 545 and 666 cm^{-1} are shift towards lower energy region with heat intensification, what can be related to difications in the [NbO$_6$] octahedra and with the formation of new Nb–O–Nb bonds. Shifts observed for the sample treated at 250 °C in comparison to the original material indicate that dehydroxylation already started at about this temperature value, in agreement with XRD results.

Figure 5 presents TGA-DTG (A) and DSC-MS (B) curves of the $H_xK_{(4-x)}Nb_6O_{17}$ sample in which four main mass loss events are observed (Fig. 5a). The first and second endothermic events occurring from room temperature up to 130 °C and in the $130 - 230$ °C range are related to the release of superficially adsorbed and intercalated water molecules (Fig. 5b, MS curve of the fragment $m/z = 18$). The third (at about $230 - 310$ °C) and fourth (in $310 - 600$ °C range) mass loss events can be related to the dehydroxylation of the dehydrated matrix by the condensation of -OH terminal groups originated from the bond established between the

interlayer H$^+$ and the niobyl (Nb=O) group, promoting the formation of new chemical bonds.

The thermal decomposition of the $H_xK_{(4-x)}Nb_6O_{17}$ material can be expressed by Eq. 1 (Bizeto and Constantino, 2004).

Table 1 presents the detailed mass loss percentages from TGA results (Fig. 5) related to the $H_xK_{(4-x)}Nb_6O_{17}$ sample, as well as the number of mols of released water molecules in the four mass loss events. For all samples, the third mass loss event is the less pronounced and initiates at around 230 °C.
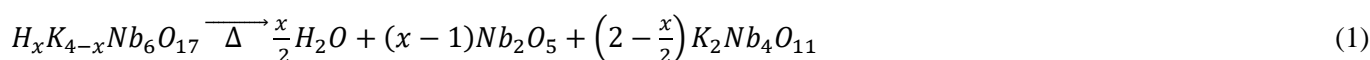

Figure 4. Raman spectra of $H_xK_{(4-x)}Nb_6O_{17}$ sample and the products isolated after the thermal treatment at 250, 300, 350, and 400 °C.
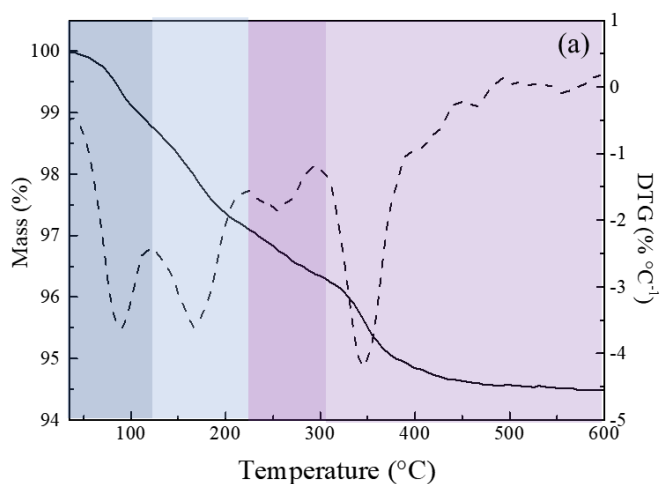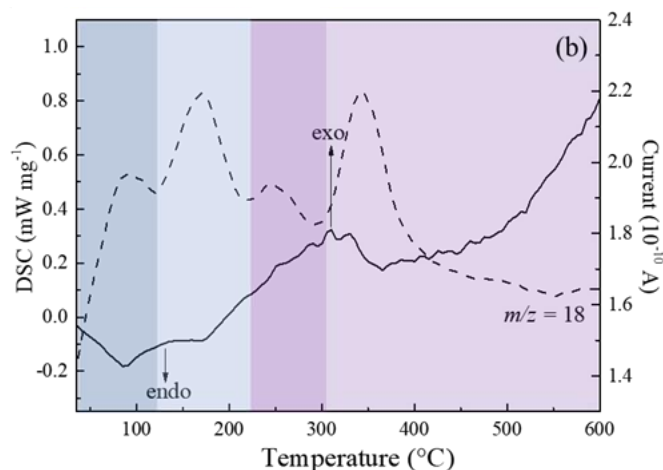
Figure 5. TGA (solid line) and DTG (dashed line) **(a)** and DSC (solid line) and MS (dashed line) **(b)** curves of $H_xK_{(4-x)}Nb_6O_{17}$ sample.

Table 1. DTG peaks, mass loss percentages for the respective temperature ranges of TGA mass loss events for the $H_xK_{(4-x)}Nb_6O_{17}$ material and the amount of released water molecules.

Temperature range (°C)	DTG peak (°C)	Δ% mass	Amount of released water (mol)
25-130	88	1.37	0.71
130-230	166	1.52	0.78
230-310	256	0.84	0.44
310-600	347	1.80	0.92

Table 2 shows the proton exchange percentages calculated from TGA (Tab. 1), considering only the fourth or both third and fourth mass loss events, and the exchange percentages obtained from ICPAES analyses of potassium, considering the Eq. 1.

$$H_xK_{4-x}Nb_6O_{17} \xrightarrow{\Delta} \frac{x}{2}H_2O + (x-1)Nb_2O_5 + \left(2 - \frac{x}{2}\right)K_2Nb_4O_{11}$$ (1)

Table 2. Proton exchange percentages calculated from TGA and ICP-AES data

4° TGA mass loss event (%)	3° and 4° TGA mass loss event (%)	ICP – AES (%)
45.8	68.0	64.0

From results displayed in Tab. 2, considering only the fourth mass loss event for the calculation of the proton exchange percentage, the value is close to 50% (45.8%). Bizeto and Constantino (2004) calculated the exchange percentage for the $H_xK_{(4-x)}Nb_6O_{17}$ sample prepared by suspending the $K_4Nb_6O_{17}$ phase in 6 mol L^{-1} HNO_3 solution at 60 °C for three days. In that work, it was considered that the dehydroxylation occurs from 315 °C. Thus, the last TGA mass loss event was considered for the calculation of ion exchange percentage, resulting in about 50%. However, when considered here both the third and the fourth events corresponding to the dehydroxylation, proton exchange percentage was much higher (68.0%) and closer to that one observed from ICP-AES quantification (64.0%). Thus, regions I and II were hydrated and could undergo the exchange of K^+ by H^+ ion.

In this work, the hexaniobate dehydroxylation process was studied for a more precise determination of its starting temperature, shown to be below 300 °C. Accordingly, the quantification of K^+ cations by ICP-AES endorsed the necessity to consider both third and fourth mass loss events for the determination of the extension of the proton exchange reaction from TGA analysis. Moreover, results presented here indicate that region II can also be hydrated in a meaningful amount and experience the intercalation of H^+ cations. Acid phase obtained under mild experimental conditions reported in this study can be expressed as $H_{2.7}K_{1.3}Nb_6O_{17}$ or $H_{2.6}K_{1.3}Nb_6O_{17}$, calculated from TGA and ICP-AES, respectively.

4. Conclusions

The XDR patterns confirmed the formation of the $K_4Nb_6O_{17}·3H_2O$ and $H_xK_{(4-x)}Nb_6O_{17}$ phases. From ICP-AES results, proton exchange was equal to 64.0%. Comparatively, results from TGA indicated 45.8% and 68.0% of proton exchange when considered hydroxylation event above 230 or 310 °C, respectively. These analytical data, combined to the XRD and Raman spectroscopic analyses of the acid hexaniobate heated from 250 to 400 °C, indicate that dehydroxylation process starts around 230 °C. Region II can also be hydrated and have K^+ cations exchanged by H^+. TGA-MS is a suitable tool to determine the level of protonation of hexaniobate, assisting the investigation of experimental approaches to improve the niobate exfoliation, such as ultrasonication, because exfoliation depends on the reactivity of the acidic intermediate phase.

Authors' contribution

Conceptualization: Constantino, V. R. L.
Data curation: Figueiredo, M. P.; Constantino, V. R. L.
Formal Analysis: Figueiredo, M. P.
Funding acquisition: Constantino, V. R. L.

Investigation: Figueiredo, M. P.
Methodology: Figueiredo, M. P.; Constantino, V. R. L.
Project administration: Constantino, V. R. L.
Resources: Constantino, V. R. L.
Software: Not applicable.
Supervision: Constantino, V. R. L.
Validation: Figueiredo, M. P.
Visualization: Figueiredo, M. P.
Writing – original draft: Figueiredo, M. P.
Writing – review & editing: Figueiredo, M. P.; Constantino, V. R. L.

Data availability statement

All data sets were generated or analyzed in the current study.

Funding

Acknowledgments

References

Bizeto, M. A; Constantino, V. R. L.; Structural Aspects and Thermal Behavior of the Proton Exchanged Layered Niobate $K_4Nb_6O_{17}$. *Mater. Res. Bull.* **2004**, *39* (11), 1729–1736. https://doi.org/10.1016/j.materresbull.2004.05.001

Bizeto, M. A.; Christino, F. P.; Tavares, M. F. M.; Constantino, V. R. L. Aspectos estruturais relacionados ao processo de troca iônica no niobato lamelar $K_4Nb_6O_{17}$. *Quim. Nova.* **2006**, *29* (6), 1215-1220. https://doi.org/10.1590/S0100-40422006000600013

Bizeto, M. A.; Shiguihara, A. L.; Constantino, V. R. L. Layered niobate nanosheets: building blocks for advanced materials assembly. *J. Mater. Chem.* **2009**, *19* (17), 2512–2525. https://doi.org/10.1039/b821435b

Bizeto, M. A.; Leroux, F.; Shiguihara, A. L.; Temperini, M. L. A.; Sala, O.; Constantino, V. R. L. Intralamellar structural modifications related to the proton exchanging in $K_4Nb_6O_{17}$ layered phase. *J. Phys. Chem. Solids.* **2010**, *71* (4), 560–564. https://doi.org/10.1016/j.jpcs.2009.12.036

Elumalai, S.; Vadivel, S.; Yoshimura, M. Interlayer-modified two-dimensional layered hexaniobate $K_4Nb_6O_{17}$ as an anode material for lithium-ion batteries. *Mater. Adv.* **2021**, *2* (6), 1957–1961. https://doi.org/10.1039/D1MA00055A

Gasperin, M.; Le Bihan, M.-T. Un niobate de rubidium d'un type structural nouveau: $Rb_4Nb_6O_{17}\cdot 3H_2O$. *J. Solid State Chem.* **1980**, *33* (1), 83–89. https://doi.org/10.1016/0022-4596(80)90550-2

Gasperin, M.; Le Bihan, M.T. Mecanisme d'hydratation des niobates alcalins lamellaires de formule $A_4Nb_4O_{17}$ (A = K, Rb, Cs). *J. Solid State Chem.* **1982**, *43* (3), 346–353. https://doi.org/10.1016/0022-4596(82)90251-1

Guo, C.; Zhu, J.; He, J.; Hu, L.; Zhang, P.; Li, D. Catalytic oxidation/photocatalytic degradation of ethyl mercaptan on α-MnO_2@$H_4Nb_6O_{17}$-NS nanocomposite. *Vacuum.* **2020**, *182*, 109718. https://doi.org/10.1016/j.vacuum.2020.109718

Hu, C.; Zhang, L.; Cheng, L.; Chen, J.; Hou, W.; Ding, W. A comparison of H^+-restacked nanosheets and nanoscrolls derived from $K_4Nb_6O_{17}$ for visible-light degradation of dyes. *J. Energy Chem.* **2014**, *23* (2), 136–144. https://doi.org/10.1016/S2095-4956(14)60128-5

Kimura, N.; Kato, Y.; Suzuki, R.; Shimada, A.; Tahara, S.; Nakato, T.; Matsukawa, K.; Mutin, P.H.; Sugahara, Y. Single- and Double-Layered Organically Modified Nanosheets by Selective Interlayer Grafting and Exfoliation of Layered Potassium Hexaniobate. *Langmuir.* **2014**, *30* (4), 1169–1175. https://doi.org/10.1021/la404223x

Li, D.; Li, Q.; He, J.; Hu, L.; Hu, J. Niobate nanoscroll composite with Fe_2O_3 particles under moderate conditions: assembly and application research. *New J. Chem.* **2016**, *40* (1), 136–143. https://doi.org/10.1039/C5NJ02120K

Liu, X.; Que, W.; Chen, P.; Tian, Y.; Liu, J.; He, Z.; Zhou, H.; Kong, L. B. Facile preparation of protonated hexaniobate nanosheets and its enhanced photocatalytic activity. *Nanotechnology.* **2017**, *28* (23), 235702. https://doi.org/10.1088/1361-6528/aa6b4f

Madaro, F.; Sæterli, R.; Tolchard, J.; Einarsrud, M.-A.; Holmestad, R.; Grande, T. Molten salt synthesis of $K_4Nb_6O_{17}$, $K_2Nb_4O_{11}$ and KNb_3O_8 crystals with needle- or plate-like morphology. *CrystEngComm.* **2011**, *13* (5), 1304–1313. https://doi.org/10.1039/C0CE00413H

Maeda, K.; Eguchi, M.; Lee, S.-H. A.; Youngblood, W. J.; Hata, H.; Mallouk, T. E. Photocatalytic Hydrogen Evolution from Hexaniobate Nanoscrolls and Calcium Niobate Nanosheets Sensitized by Ruthenium(II) Bipyridyl Complexes. *J. Phys. Chem. C.* **2009**, *113* (18), 7962–7969. https://doi.org/10.1021/jp900842e

Müller-Warmuth, W.; Schöllhorn, R. Progress in Intercalation Research. In *Physics and Chemistry of Materials with Low-Dimensional Structures*; Springer, 1994.

Nassau, K.; Shiever, J. W.; Bernstein, J. L. Crystal Growth and Properties of Mica-Like Potassium Niobates. *J. Electrochem. Soc.* **1969**, *116* (3), 348–353.

Rao, C. N. R.; Raveau, B. *Transition Metal Oxides: Structure, Properties, and Synthesis of Ceramic Oxides*. Wiley, 1998.

Shiguihara, A. L.; Bizeto, M. A.; Constantino, V. R. L. Exfoliation of layered hexaniobate in tetra(n-butyl)ammonium hydroxide aqueous solution. *Colloids Surf. A: Physicochem. Eng. Asp.* **2007**, *295* (1–3), 123–129. https://doi.org/10.1016/j.colsurfa.2006.08.040

Shiguihara, A.; Bizeto, M. A.; Constantino, V. R. L. Chemical modification of niobium layered oxide by tetraalkylammonium intercalation. *J. Braz. Chem. Soc.* **2010**, *21* (7), 1366–1376. https://doi.org/10.1590/S0103-50532010000700024

Silva, C. H. B.; Iliut, M.; Muryn, C.; Berger, C.; Coldrick, Z.; Constantino, V. R. L., Temperini, M. L. A., Vijayaraghavan, A. Ternary nanocomposites of reduced graphene oxide, polyaniline and hexaniobate: Hierarchical architecture and high polaron formation. *Beilstein J. Nanotechnol.* **2018**, *9*, 2936–2946. https://doi.org/10.3762/bjnano.9.272

Wei, Q.; Nakato, T. Preparation of a layered hexaniobate–titania nanocomposite and its photocatalytic activity on removal of phenol in water. *J. Porous. Mater.* **2009**, *16* (2), 151–156. https://doi.org/10.1007/s10934-007-9179-2